ChemSusChem

Supporting Information

Tailoring the Performance of ZnO for Oxygen Evolution by Effective Transition Metal Doping

Qiuhua Liang, Geert Brocks,* Vivek Sinha, and Anja Bieberle-Hütter*

1. Electronic properties of pristine and TM doped ZnO

In Sec 1.1 we analyze the electronic structure of bulk ZnO and the ZnO surface, as calculated with DFT, using the GGA/PBE and GGA/PBE+*U* functionals. We conclude that introducing on-site Coulomb interaction through *U* can improve the description of the ZnO band gap, but a significant improvement is only achieved at the cost of worsening the lattice parameters.

In Sec 1.2, we characterize the electronic structure of TM doped ZnO. We establish the high-spin character of the 3d TM dopant ions, having a local atomic configuration $3d^n$ and a valency of 2+. The high-spin character of the late TM dopants Mn, Fe, Co, Ni, and Cu is not affected by the incorrect DFT band gap.

1.1 GGA and GGA+*U* calculations for ZnO

We start by analyzing the electronic structure of the ZnO slab, terminated by $(10\bar{1}0)$ surface, see Figure 1 of the main text. The projected densities of states (PDOS), projected on the Zn and O atoms, are shown in Figure S1. Calculated with the GGA/PBE functional, bulk ZnO is a semiconductor with a band gap of 0.8 eV, and the ZnO slab has the same calculated gap, demonstrating the absence of surface states in the gap region. The calculated band gap is much smaller than the experimental value of 3.4 eV,[1] but is in agreement with the band gap found in previous DFT studies.[2] It is well known that standard GGA functionals severely underestimate the band gap ZnO.[2-3]

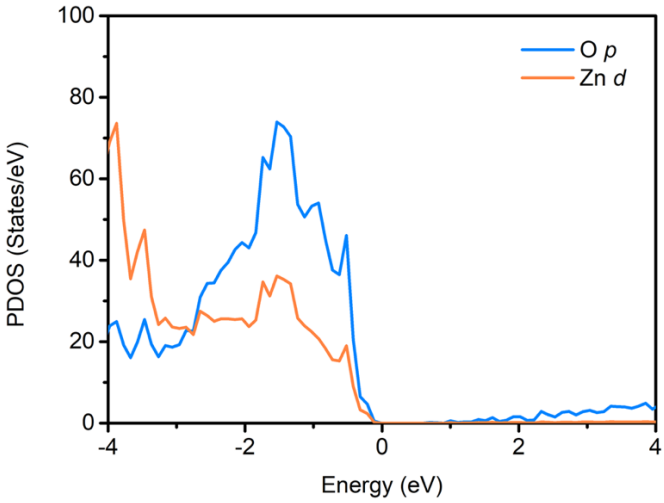

Figure S1. Projected densities of states (PDOS) of the pristine ZnO slab.

Following the literature,[4] we have explored enlarging the calculated band gap using the GGA+*U* technique within the Dudarev et al. approach.[4a] It is quite common to treat 3d TMs adding on-site Coulomb and exchange parameters *U* and *J*. In addition, as both the top of the valence band, as well as the bottom of the conduction band of ZnO have considerable O character, see Figure S1, it requires the use of such on-site parameters for the O atoms, in order to be able to influence the size of the band gap, although this may seem somewhat unphysical. We have tested the PBE+*U* functional with two sets of $U-J$ parameters on both the Zn atoms, as well as on the O atoms: (a) $(U-J)_{\mathrm{Zn}}=8$ eV for Zn 3d states and $(U-J)_{\mathrm{O}}=10$ eV for O 2p states, according to ref. 4, and (b) $(U-J)_{\mathrm{Zn}}=6$ eV for Zn 3d states and $(U-J)_{\mathrm{O}}=15$ eV for O 2p states, according to ref.[4b]. The calculated band structures are shown in Figure S2.

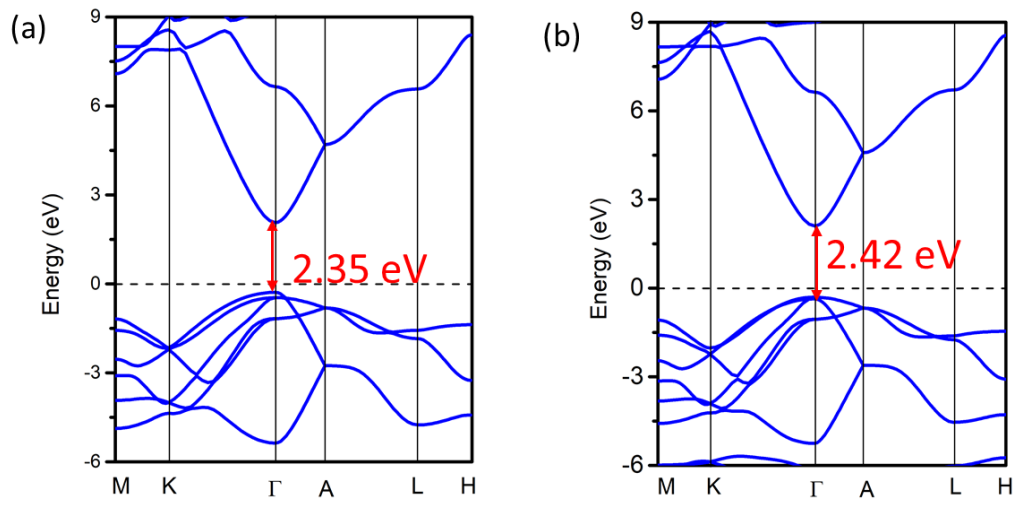

Figure S2. Calculated band structures of bulk ZnO: (a) $(U-J)_{\mathrm{Zn}}=8$ eV for Zn 3d states and $(U-J)_{\mathrm{O}}=10$ eV for O 2p states; (b) $(U-J)_{\mathrm{Zn}}=6$ eV for Zn 3d states and $(U-J)_{\mathrm{O}}=15$ eV for O 2p states.

It is observed that adding $U-J$ enlarges the band gap of ZnO significantly, from 0.8 eV to 2.4 eV, but the values obtained are still much smaller than the experimental band gap of 3.4 eV.[1] Moreover, the $U-J$ values used for O in particular already seem to be unphysically large. It is possible to approach the experimental band gap, but only at the cost of enlarging these values even further. Following ref. 6, we have increased the $U-J$ values to $(U-J)_{\mathrm{Zn}}=13$ eV for Zn 3d states and $(U-J)_{\mathrm{O}}=20$ eV for O 2p states, which increases the calculated ZnO band gap to 3.2 eV, see Figure S3(a). All

these calculations have been done using the standard VASP PAW potentials for Zn (12 valence electrons) and O (6 valence electrons). We have also explored the use of the *GW*-type PAW potentials Zn_sv_*GW* (20 valence electrons) and O_*GW* (6 valence electrons), but that decreases the band gap again to 2.9 eV, as shown in Figure S3(b).

In conclusion, it is possible by using GGA+*U* to obtain a calculated band gap that is close to the experimental value. However, it also involves the use of unphysically large values of $U-J$, which has undesirable side effects in the structure of ZnO. Optimizing the ZnO lattice parameters with $(U-J)_{\mathrm{Zn}}=13$ eV and $(U-J)_{\mathrm{O}}=20$ eV gives *a* = 3.16 Å and *c* = 5.06 Å with standard PAW potentials, and *a* = 3.17 Å and *c* = 5.07 Å with *GW*-type PAW potentials. These values are ~3% smaller than the experimental values of *a* = 3.25 Å and *c* = 5.21 Å.[4b] In contrast, the standard PBE functional gives optimized lattice parameters $a=3.28$ Å, $c=5.30$ Å, which are in much better agreement with experiment.

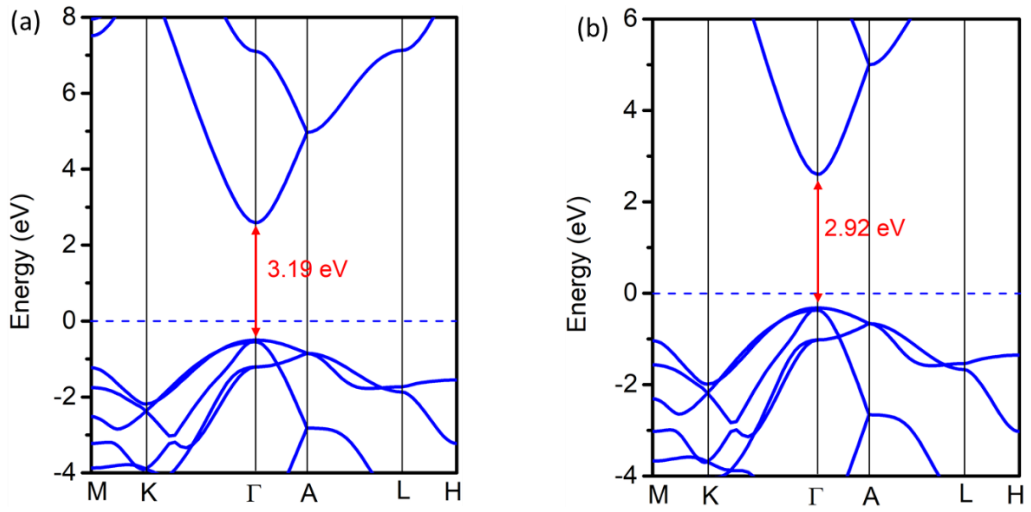

Figure S3. Calculated band structures of bulk ZnO with $(U-J)_{\mathrm{Zn}}=13$ eV for Zn 3d states and $(U-J)_{\mathrm{O}}=20$ eV for O 2p states: (a) with standard Zn (12 valence electrons) and O (6 valence electrons) PAW potentials; (b) with Zn_sv_*GW* (20 valence electrons) and O_*GW* (6 valence electrons) PAW potentials.

1.2 GGA and GGA+*U* calculations for TM doped ZnO

Doping the ZnO slab discussed in the previous section with one TM atom at the $(10\bar{1}0)$ surface position, as discussed in the main text, leads to the PDOSs shown in Figure S4, calculated with the spin-polarized GGA/PBE functional. One observes the

emergence of localized 3d states of the TM atoms. Going down the TM series from Sc to Cu, these 3d states monotonically decrease in energy. For Sc, all the 3d states are unoccupied and coincide with the conduction band of ZnO, giving Sc the configuration $3d^0$. For Cu all the 3d states are occupied and coinciding with the ZnO valence band, except for one spin-down state that is empty and just above the valence band, giving Cu the configuration $3d^9$. The elements between Sc and Cu then have configuration $3d^n$, where *n* is the number of *d* electrons of the neutral TM atom.

Starting with a neutral TM atom with configuration $4s^2 3d^n$, we then conclude that substituting one Zn atom by a TM atom, two electrons are donated by the TM 4s shell to arrive at a charge 2+, and, thus, the nominal charge of a TM substitutional dopant atom in the ZnO slab is 2+.

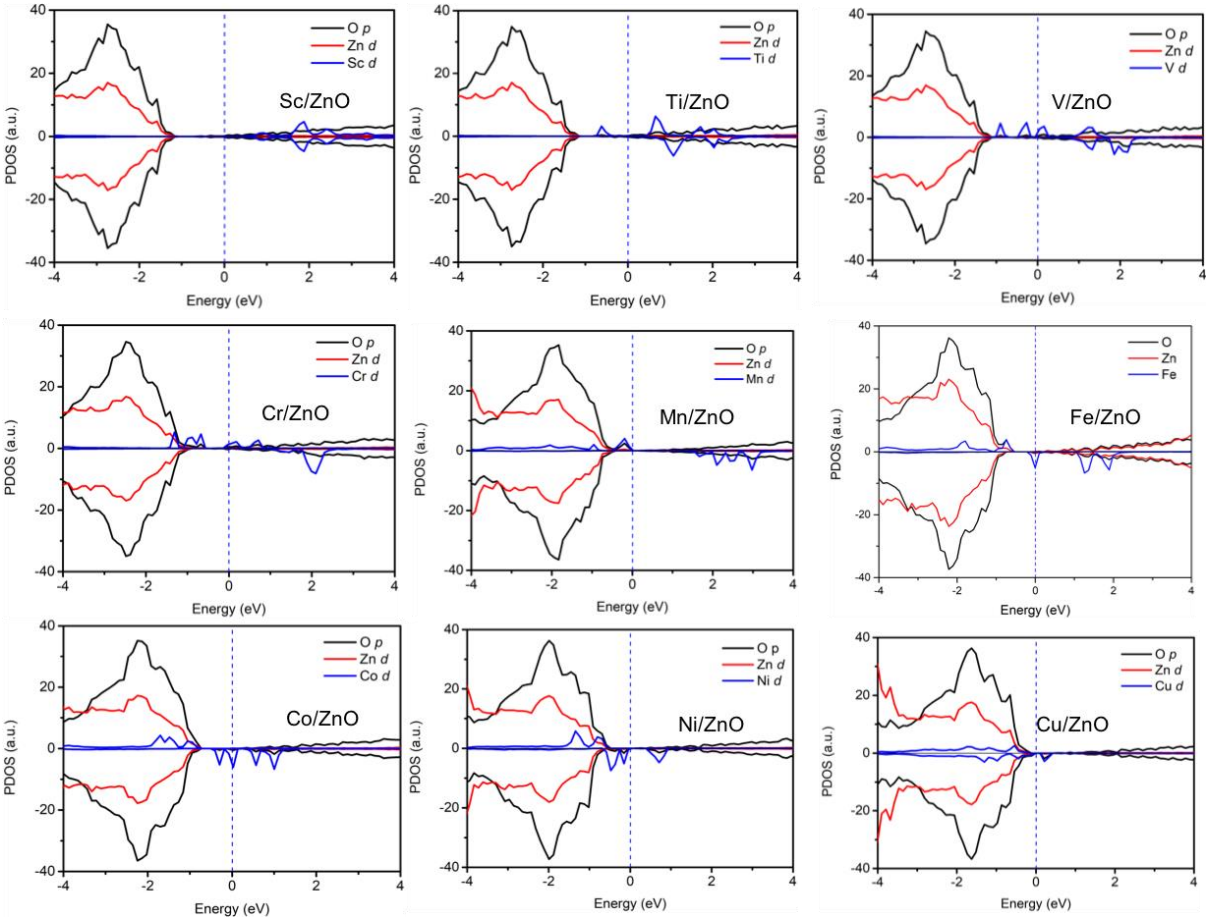

Figure S4. Projected densities of states (PDOS) of the ZnO slab, doped with one TM atom.

We can test this analysis by calculating the magnetic moments of the TM doped ZnO slab. As a reference, the magnetic moments of isolated TM^{2+} ions of

configuration $4s^0 3d^n$ in their high-spin states are given in the first row of Table S1, and the magnetic moments of the TM doped ZnO slab are given in the second row. It can be observed that the late TM dopant atoms, from Mn to Cu, all have magnetic moments equal to the high-spin state of their corresponding TM^{2+} ions

The calculated magnetic moments of the early TM dopant atoms, Sc to Cr, are all significantly smaller than those of their corresponding TM^{2+} high-spin ions. The PDOSs of Figure S4 show why this is the case. The TM dopant states overlap with the ZnO conduction band, and transfer electrons to the conduction band, thereby losing some of their magnetic moment. As the ZnO band gap calculated with GGA/PBE is much too small, see the previous section, this electron transfer is likely an artefact, and this functional does not properly describe the electronic configuration of the Sc to Cr dopants.

Table S1. Calculated magnetic moments of the TM doped ZnO slab (in μ_B per supercell), compared to the maximum magnetic moment of the isolated atom.

Dopants	**Sc**	**Ti**	**V**	**Cr**	**Mn**	**Fe**	**Co**	**Ni**	**Cu**
$\boldsymbol{3d^n}$	1	2	3	4	5	6	7	8	9
Atomic	1.00	2.00	3.00	4.00	5.00	4.00	3.00	2.00	1.00
Calculated	0.00	0.75	2.03	3.49	5.00	4.00	3.00	2.00	1.00

We test whether the PBE+*U* functional improves this description. The magnetic moments of the TM-doped ZnO slab, calculated with the PBE+*U* functional, using the same parameter settings as in Fig S2, as shown in Table S2 for the TM dopants Sc to Cr. Comparison to the results shown in Table S1 demonstrates that enlarging the band gap of ZnO using the PBE+*U* functional actually changes the magnetic moments very little.

Table S2. The calculated magnetic moment of the TM doped ZnO slab (in μ_B per supercell.

Systems	**With U_{Zn_d}= 8 eV, U_{O_p}= 10 eV, single point calculations**	**With U_{Zn_d}= 6 eV, U_{O_p}= 15 eV, single point calculations**

	Magnetic moment	Magnetic moment
Sc/ZnO	0.00	0.00
Ti/ZnO	0.71	0.72
V/ZnO	2.23	2.22
Cr/ZnO	3.50	3.50

2. OER on single TM doped ZnO

In Sec 2.1, we discuss the zero-point energy and the entropy terms, which are required to calculate the Gibbs free energies of the OER steps, see Eqs (7)-(10) in the main text.

In the main text we have only discussed the total energies of the adsorbed species in their most stable structures. For all adsorbed species, there are other metastable adsorbed structures with a slightly higher energy. For completeness, all structures and their total energies are listed and discussed in Sec 2.2 and 2.3, respectively.

In Sec 2.4, we discuss the possible influence of potential and pH on the ZnO $(10\bar{1}0)$ surface.

Calculated magnetic moments of the slab with the adsorbed species are discussed in Sec 2.5, clearly showing that the TM dopant atoms remain in their high-spin state during all the steps of the OER. Adsorption of OH or OOH increases the nominal valency of the TM dopant from 2+ to 3+, whereas adsorption of O increases it to 4+.

For completeness, calculated Bader charges of the atoms of the TM doped ZnO slab and of the adsorbed species of the OER intermediates are given in Sec 2.6.

2.1 Zero-point energy and entropic correction

Zero-point energies (ZPE) and entropic terms (*TS*) at *T* = 298 K are listed in Table S3 for the molecules in the gas phase, H_2O, H_2, and O_2, and for the adsorbed species, *OH, *O and *OOH. The values for the H_2O, H_2, and O_2 molecules in the gas phase are taken from Ref.[5] The ZPE and *TS* values of the adsorbed species are determined from the vibrational frequencies as discussed in the main text. The same values of ZPE and *TS* are used for all systems, as they are not very dependent on the details of the bonding.[6]

Table S3. Zero-point energies (ZPE) and entropic corrections (*TS*) at *T* = 298 K for the molecules in the gas phase, H_2O, H_2, and O_2, and for the adsorbed species, *OH, *O and *OOH. The values for the molecules in the gas phase are taken from Ref .[5]

Species	ZPE (eV)	TS (eV)
H_2O	0.56	0.67
H_2	0.27	0.41
O_2	0.10	0.64
*OH	0.37	0.07
*O	0.06	0.05
*OOH	0.44	0.13

2.2 Structures of OER intermediates adsorbed on the ZnO $(10\bar{1}0)$ surface

Figure S5 shows the optimized structures of the OH and O species adsorbed at an on-top position on a TM doped surface. Adsorption at a bridge site position is shown in Figure 1 in the main text. Figure S6 shows the optimized structures of the OOH species adsorbed on a TM doped ZnO $(10\bar{1}0)$ surface, with the TM in (a) a surface, and (b) a subsurface position, respectively. All these bonding configurations are locally stable.

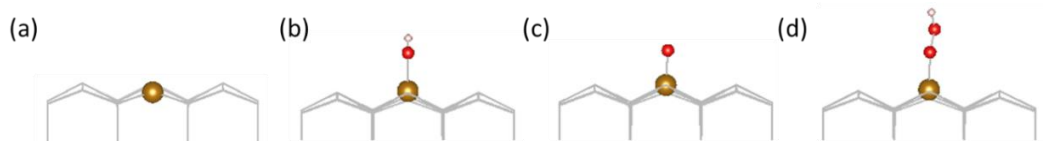

Figure S5. Side views of the atomic structures of the (a) free site, and (b) OH, (c) O and (d) OOH adsorbed at the on-top site of the TM doped ZnO $(10\bar{1}0)$ surface. The color coding is as follows: grey - Zn, brown - TM, red - O, and white - H.

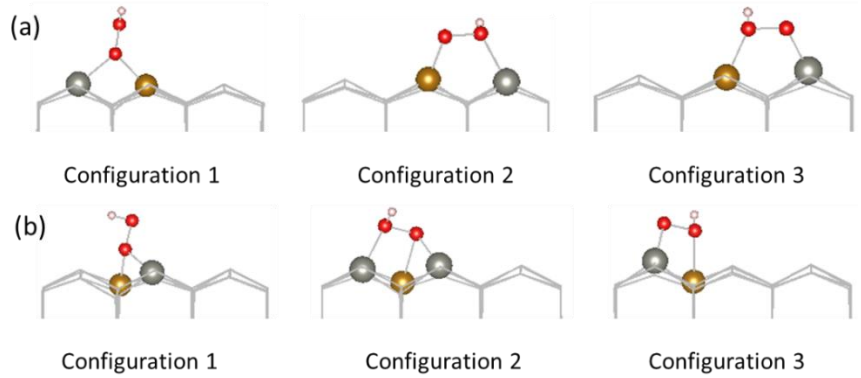

Figure S6. Side views of the atomic structures of three *OOH configurations adsorbed at bridge sites of the TM doped ZnO $(10\bar{1}0)$ surface, with the TM at (a) surface and (b) subsurface positions. Configuration 2 has the lowest total energies for all TM dopants.

2.3 Total energies of TM doped and pristine ZnO $(10\bar{1}0)$ surface vs. subsurface with/without adsorbants

Tables S4 and S5 list the total energies calculated for the TM doped and pristine ZnO surface with and without adsorbants in the structures given in Figure 1 of the main text, and Figures S4 and S5 of Sec 2.2. For those OER intermediates that adsorb at a top site, Fig S5, all their energies are higher than for adsorption at a bridge site, Figure 1 main text. For OOH the energies of all configurations of Figure S6 are listed. For configurations that do not lead to a locally stable minimum, the entries are marked with "/".

Table S4. The total energies (in eV) of the OH, O, and OOH species adsorbed at top sites and bridge sites of the TM doped ZnO $(10\bar{1}0)$ surface, where the TM is at a surface position.

Systems	Top site	Bridge site	*OOH in configuration 1	*OOH in configuration 2	*OOH in configuration 3
Mn	-532.19	-532.19			
Mn_OH	-543.46	-543.46			
Mn_O	-538.74	-538.79			
Mn_OOH	-547.46		-543.43	-547.60	-547.27
Fe	-530.87	-530.87			
Fe_OH	-541.84	-541.85			
Fe_O	-536.66	-536.81			
Fe_OOH	-545.94		-545.86	-546.13	-545.71
Co	-528.89	-528.89			
Co_OH	-539.44	-539.49			
Co_O	-534.28	-534.34			
Co_OOH	-543.70		-543.63	-543.86	-543.46
Ni	-527.13	-527.13			
Ni_OH	-537.20	-537.35			
Ni_O	-531.83	-531.88			
Ni_OOH	-541.58		-541.50	-541.67	-541.46
Cu	-525.21	-525.21			
Cu_OH	-534.66	-534.97			
Cu_O	-529.11	-529.24			
Cu_OOH	-539.15		-539.12	-539.24	-538.99
pristine ZnO	-524.55	-524.55			

ZnO_OH	-533.71	-534.05			
ZnO_O	-527.63	-528.04			
ZnO_OOH	-538.32		-538.20	-538.32	-538.31

Table S5. The total energies (in eV) of the OH, O, and OOH species adsorbed at top sites and bridge sites of the TM doped ZnO $(10\bar{1}0)$ surface, where the TM is at a subsurface position.

Systems	bridge site	*OOH in configuration 1	*OOH in configuration 2	*OOH in configuration 3
Mn	-532.22			
Mn_OH	-543.28			
Mn_O	-538.37			
Mn_OOH		-547.26	-547.39	-547.11
Fe	-530.79			
Fe_OH	-541.79			
Fe_O	-536.71			
Fe_OOH		-545.80	-546.04	-545.77
Co	-528.74			
Co_OH	-539.35			
Co_O	-534.07			
Co_OOH		-543.41	-543.53	-543.33
Ni	-526.63			
Ni_OH	-537.01			
Ni_O	-531.54			
Ni_OOH		-541.07	-541.26	-541.11
Cu	-524.73			
Cu_OH	-534.53			
Cu_O	-528.80			
Cu_OOH		-538.75	-538.72	-538.75

pristine ZnO	-524.55			
ZnO_OH	-533.83			
ZnO_O	-527.76			
ZnO_OOH	/	/	/	

2.4 OH coverage and Pourbaix diagram

In alkaline media, the ZnO surface will likely be partially hydroxylated. The stability of (partially) hydroxylated surfaces can be illustrated by a Pourbaix diagram, see Refs.[7], which depicts the most stable state of the surface as a function of the pH and of the potential *U*. We have looked specifically at the ZnO $(10\bar{1}0)$ surface with hydroxyl (OH) groups adsorbed on the Zn atoms at the surface, in coverages of 1/6 ML OH, 1/3 ML OH, 1/2 ML OH, and 2/3 ML OH. Figure S7 shows the calculated Pourbaix diagram for these coverages. It demonstrates that ZnO is not covered at a low potential under all pH, and that the OH coverage increases with increasing potential. A large coverage, which could influence the OER mechanism, is not reached for realistic *U*/pH combinations.

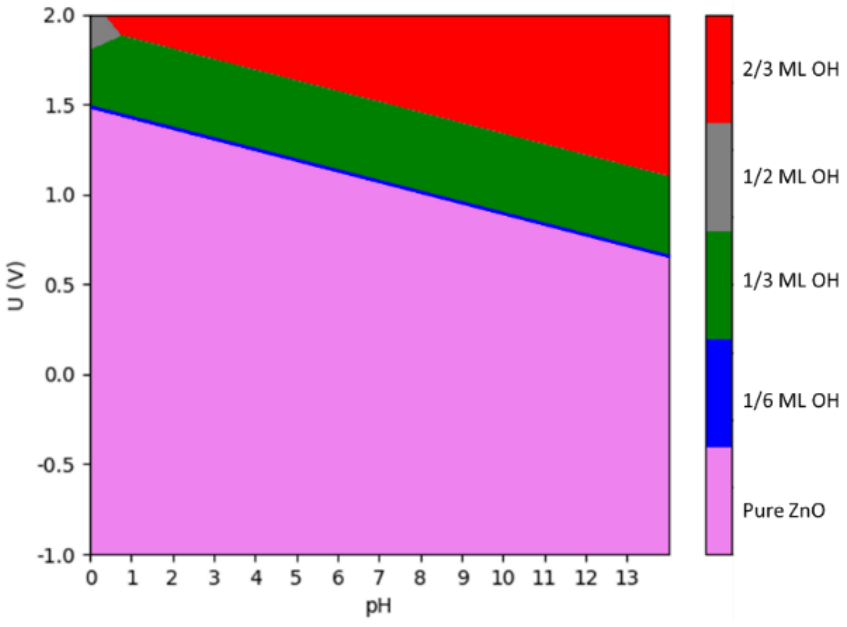

Figure S7. Pourbaix diagram, indicating the thermodynamically stable OH coverage of the ZnO $(10\bar{1}0)$ surface as a function of pH and potential *U*.

2.5 Magnetic moments of TMs doped ZnO

Table S6 lists the total magnetic moments of the TM doped ZnO slab with and without adsorbants. All TM dopant atoms remain in their high-spin state.

Table S6. Calculated total magnetic moments (in μ_B per Supercell) of TM doped ZnO.

system	Mn	Fe	Co	Ni	Cu
Nothing adsorbed	5	4	3	2	1
OH adsorbed	4	5	4	3	2
O adsorbed	3	4	5	4	3
OOH adsorbed	4	5	4	3	2

2.6 Bader charges of TMs doped ZnO surface

Table S7 shows the Bader charges of the atoms in the TM doped ZnO surface and of the oxygen atoms of adsorbed species for the different OER steps. For the pristine ZnO system, the given charge is the average of all the Zn atoms. The charges of the oxygen ions of all adsorbed species were calculated for all geometries.

Table S7. Calculated Bader charges (in μ_B per Supercell) of TM doped ZnO.

Systems	TM	Zn	HO_{ads}	O_{ads}	HOO_{ads}-TM	HOO_{ads}-Zn
Mn	1.25	1.16				

Mn_OH	1.51	1.22	-1.13			
Mn_O	1.59	1.22		-0.81		
Mn_OOH	1.52	1.21			-0.49	-0.60
Fe	1.16	1.16				
Fe_OH	1.53	1.23	-1.16			
Fe_O	1.53	1.23		-0.77		
Fe_OOH	1.51	1.23			-0.49	-0.66
Co	1.03	1.17				
Co_OH	1.36	1.23	-1.15			
Co_O	1.36	1.21		-0.66		
Co_OOH	1.36	1.23			-0.45	-0.67
Ni	0.97	1.16				
Ni_OH	1.17	1.22	-1.07			
Ni_O	1.23	1.23		-0.70		
Ni_OOH	1.23	1.22			-0.40	-0.64
Cu	0.93	1.16				
Cu_OH	1.15	1.23	-1.10			
Cu_O	1.16	1.23		-0.70		
Cu_OOH	1.14	1.21			-0.39	-0.59
Zn		1.20				
Zn_OH	1.25	1.24	-1.15			
Zn_O	1.26	1.26		-0.69		
Zn_OOH	1.25	1.19			-0.32	-0.57

3. OER on double TM doped ZnO

The intermediate species involved in the OER adsorb at bridge sites on the ZnO $(10\bar{1}0)$ surface. In the case of the OH and O species, the O atom binds to the TM dopant atom in the surface as well as to a nearby Zn atom in the surface, whereas for the OOH species, one of the O atoms binds to a TM dopant atom and the other one to a nearby Zn atom, see Figure 1 in the main text. This is the most common type of bonding that will be observed if the ZnO is doped with TM at moderate or low concentrations. At high concentrations, configurations occur more often where two TM dopant atoms are relatively close, so that the adsorbed species can form bridge bonds to two TM dopants in the surface, see Figure 8 in the main text.

In Sec 3.1, we discuss possible structures of such bonding configurations, their energies and stability. In Sec 3.2, we show the Gibbs free energies of the OER steps, Eqs (7)-(10) in the main text, and the binding free energies of the OER intermediate species, Eqs (16)-(18), based upon these bonding configurations.

3.1 Surface and subsurface double doping sites

To have a catalytic effect on the OER, TM dopant atoms can substitute Zn atoms in the $(10\bar{1}0)$ surface at ridge positions or at valley positions, which we call “surface” and “subsurface” positions, respectively, see Figure 1 in the main text. Two adjacent TM dopant atoms can be both at surface positions or one at a surface position and the other one at a subsurface position, see Figure 8 in the main text. Other combinations of two adjacent TM atoms are not catalytically active. Tables S8 and S9 give the total energies of the ZnO slab containing two TM dopant atoms in two surface positions, and one surface and one subsurface position, respectively. From these results we conclude that it is energetically more advantageous to have the two TM dopant atoms both in surface positions, which is consistent with what we have found for single, isolated TM dopant atoms, see the main text. In Figure S8, we consider the stability of double TM doped ZnO. In particular, we focus on the net interaction between the TM dopants.

Table S8. The total energies of the ZnO slab doped with two TM atoms in adjacent surface positions.

Systems	Total energy (eV)
Mn	-539.79
Fe	-537.12
Co	-533.16
Ni	-529.70
Cu	-525.98

Table S9. The total energies of the ZnO slab doped with two TM atoms, one in a surface position, and one in an adjacent subsurface position.

Systems	Total energy (eV)
Mn	-539.82
Fe	-537.04
Co	-533.13
Ni	-529.38
Cu	-525.46

Figure 3 in the main text demonstrates that substituting individual Zn atoms by TM atoms leads to a stable system. Whether these point substitutions tend to cluster is investigated by focusing on the binding energy ΔE_{bind} between substitutions *A* and *B*[8]

$$\Delta E_{\mathrm{bind}} = E_A + E_B - E_{AB} - E_0,$$

where E_A, E_B are the total energies of the ZnO slab containing the substitutions *A* and *B*, respectively, E_{AB} is the total energy of the ZnO slab containing the double substitution *AB*, and E_0 is the total energy of the pristine ZnO slab. The calculated results are shown in Figure S8, where $\Delta E_{\mathrm{bind}} < 0$ indicates a net repulsion between the two dopant atoms, and $\Delta E_{\mathrm{bind}} > 0$ indicates a net attraction. The results show that in the majority of cases the binding energy is small, $|\Delta E_{\mathrm{bind}}| \lesssim 0.1$ eV, demonstrating that there is little interaction between the dopant atoms.

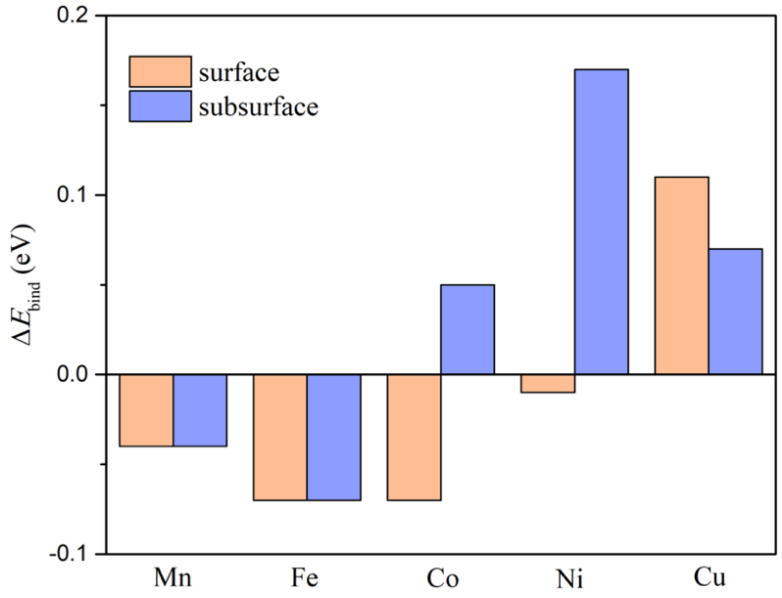

Figure S8. Binding energy ΔE_{bind} between two TM atoms, substituting two neighboring Zn atoms at $(10\bar{1}0)$ surface positions (labeled “surface”), or at one surface position and one subsurface position (labeled “subsurface”).

We consider the OER intermediates, OH, O, and OOH, adsorbed at bridge sites between two adjacent TM dopant atoms. For OOH adsorbed on two adjacent surface TM dopants, there are two stable *OOH configurations, named TM-OOH1 and TM-OOH2 in the following. For OOH adsorb on one surface and one subsurface TM dopants, there are three *OOH stable configurations, named TM-OOH1, TM-OOH2, and TM-OOH3, see Figure 8 in the main text. The total energies of the OER intermediates adsorbed on the two TM surface dopants, and on one surface and one subsurface TM dopant, are listed in Tables S10 and S11, respectively.

Table S10. The total energies of the OH, O, and OOH adsorbed on the ZnO slab doped with two TM atoms in adjacent surface positions; “/” means that the OOH does not adsorb stably in this configuration.

Systems	Total energy (eV)
Mn_OH	-551.31
Mn_O	-547.23
Mn_OOH1	-555.31
Mn_OOH2	-555.45
Fe_OH	-548.34
Fe_O	-543.58
Fe_OOH1	-552.35
Fe_OOH2	-552.26
Co_OH	-544.04
Co_O	-539.27
Co_OOH1	-548.17
Co_OOH2	-548.05
Ni_OH	-540.18
Ni_O	-535.15
Ni_OOH1	-544.36
Ni_OOH2	-544.50
Cu_OH	-535.7
Cu_O	-530.28
Cu_OOH1	-539.81
Cu_OOH2	/

Table S11. The total energies of the OH, O, and OOH adsorbed on the ZnO slab doped with two TM atoms, one in a surface position, and one in an adjacent subsurface position; “/” means that the OOH does not adsorb stably in this configuration.

Systems	Total energy (eV)
Mn_OH	-551.12
Mn_O	-546.71
Mn_OOH1	-555.06
Mn_OOH2	-555.17
Mn_OOH3	-555.23
Fe_OH	-547.98
Fe_O	-543.48
Fe_OOH1	-552.01
Fe_OOH2	-552.28
Fe_OOH3	-552.25
Co_OH	-543.74
Co_O	-538.94
Co_OOH1	-548.16
Co_OOH2	-548.03
Co_OOH3	-548.22
Ni_OH	-539.74
Ni_O	-534.61
Ni_OOH1	-543.86
Ni_OOH2	-543.93
Ni_OOH3	-544.12

Cu_OH	-535.26
Cu_O	-529.76
Cu_OOH1	/
Cu_OOH2	-539.22
Cu_OOH3	/

3.2 Gibbs free energies and overpotentials

Figure S9 shows the Gibbs free energies of the four reaction steps, Eqs (7)-(10) of the main text, calculated for the double TM doped ZnO $(10\bar{1}0)$ surface for the 3d TM atoms Mn, Fe, Co, Ni, and Cu. The overpotentials are calculated and are given in the legend. The overpotentials range from 1.71 V to 0.44 V and decrease monotonically from Mn to Cu. Mn and Fe double substitutions lead to higher overpotentials compared to pristine ZnO, see Figure 9 in the main text, whereas Ni and Cu show much lower overpotentials.

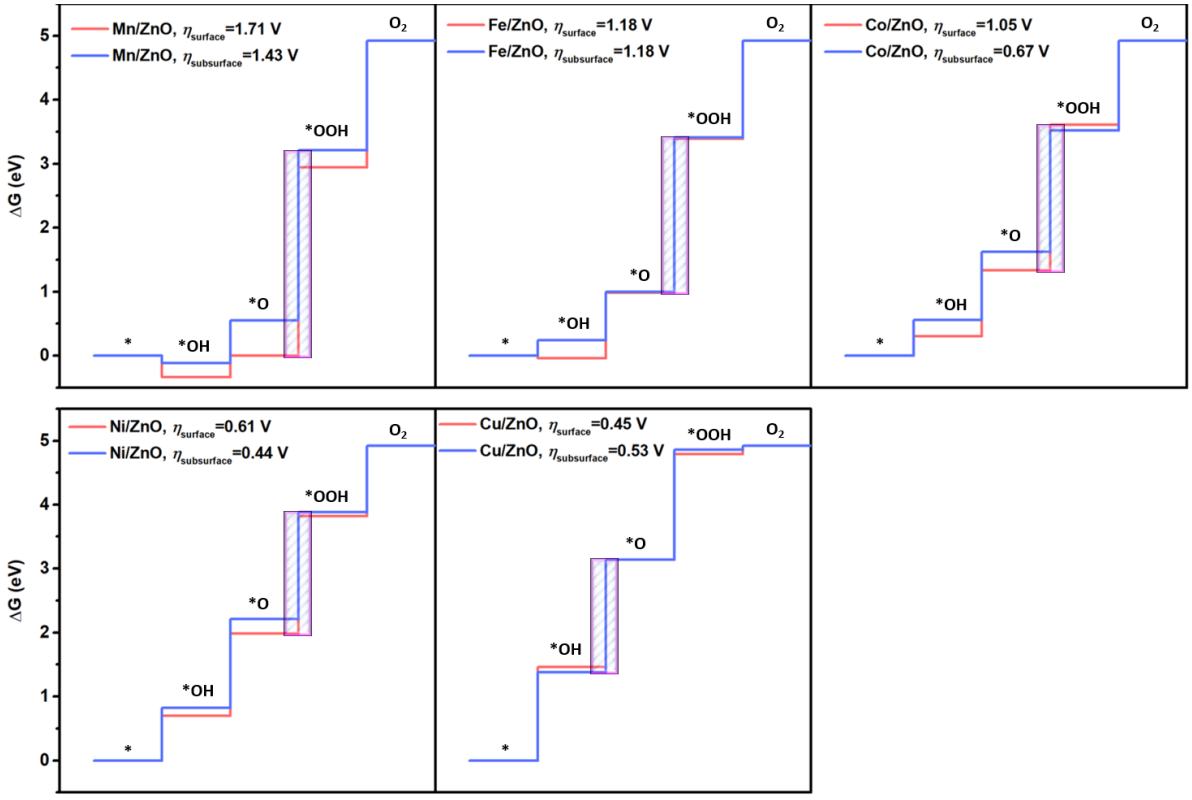

Figure S9. Gibbs free energy diagrams of double TMs doped ZnO surface and subsurface systems. The purple-shaded fields indicate the potential determining steps. The overpotentials are given in the legends; η_{surface} and $\eta_{\mathrm{subsurface}}$ represent the overpotentials of surface and subsurface, respectively.

Figures S10(a) and (b) plot the free energies of adsorption, ΔG_{*OH}, ΔG_{*O}, and ΔG_{*OOH}, Eqs (16)-(18) in the main text, of the OER intermediates as a function of the double TM dopants on surface and subsurface, respectively. The lower the free energy, the stronger the binding of the intermediates to the active site. The ΔG_{*OH}, ΔG_{*O}, and ΔG_{*OOH} show a similar trend in surface and subsurface. It is found that all free energy curves increase from Mn to Cu. ΔG_{*O} for Mn, Fe, and Co is closer to ΔG_{*OH} than that of Ni and Cu; this indicates that O is strongly bonded to the active site in the Mn, Fe, and Co systems.

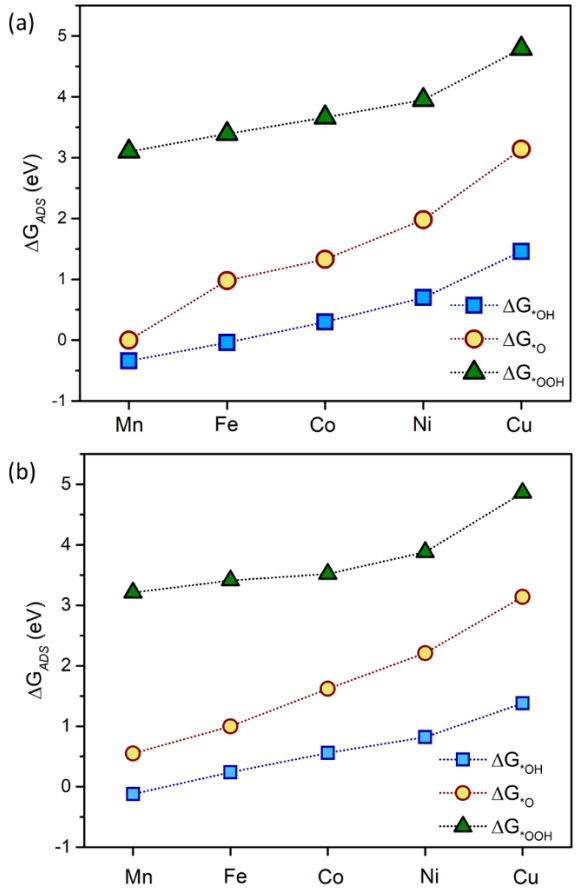

Figure S10. Gibbs free energies of the OER intermediates on double TMs doped ZnO $(10\bar{1}0)$ (a) surface and (b) subsurface. Adsorbed species is abbreviated as ADS and signifies *OH (blue squares), *O (yellow circles), and *OOH (green triangles).

4. Electrochemical-step symmetry index (ESSI)

Alternative ways to analyze the overpotential for metal electrodes make use of scaling relations to, for instance, the electrochemical-step symmetry index (ESSI).[9] Figure S11 shows the calculated overpotential η plotted against the ESSI for doped ZnO, for all TM substitutions in the single doped and double doped cases. The straight line $\eta = 1.29\ \mathrm{ESSI} + 0.14$ represents a least square fit through the data points. Although there is definitely some trend, the scaling relation is a little different from the relation $\eta = 0.99\ \mathrm{ESSI} + 0.25$ in Ref.[9] Moreover, there is also some scatter of points around the trend line. We feel that the results regarding this scaling relation does not give further insight in this case.

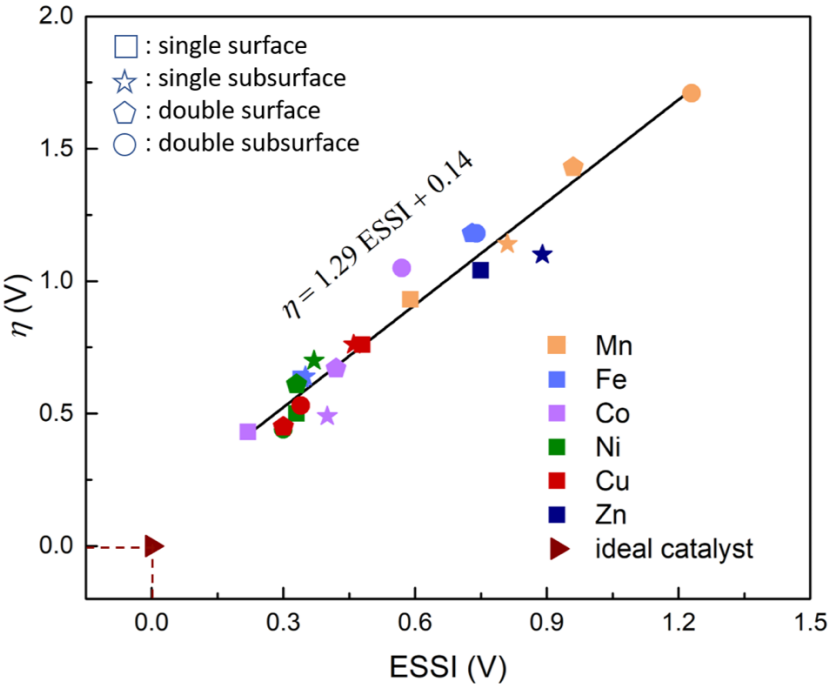

Figure S11. Overpotential η (V) plotted against the ESSI (V) for doped ZnO, for all TM substitutions in the single doped and double doped cases.

5. Lattice constants and Coordinates

The lattice constants and atomic positions of the pure and TM doped ZnO $(10\bar{1}0)$ slab, and OER intermediates adsorbed on pure and TM doped ZnO surface and subsurface during OER reaction cycle are supplied in the folder named “POSCAR”. “singleTM” and “doubleTM” in the folder “POSCAR” mean the single TM dopant and double TM dopants substitute the Zn atoms in surface or subsurface positions, respectively.

References

[1] a) K. R. Kittilstved, W. K. Liu, D. R. Gamelin, *Nat. Mater.* **2006**, *5*, 291-297; b) A. Walsh, J. L. Da Silva, S.-H. Wei, *Phys. Rev. Lett.* **2008**, *100*, 256401.

[2] C. Wang, G. Zhou, J. Li, B. Yan, W. Duan, *Phys. Rev. B* **2008**, *77*, 245303.

[3] a) Q. Lin, G. Li, N. Xu, H. Liu, D. E, C. Wang, *J. Chem. Phys.* **2019**, *150*, 094704; b) K. Bashyal, Bowling Green State University **2017**; c) K. Bashyal, C. K. Pyles, S. Afroosheh, A. Lamichhane, A. T. Zayak, *J. Phys. Condens. Matter* **2018**, *30*, 065501.

[4] a) S. Dudarev, G. Botton, S. Savrasov, C. Humphreys, A. Sutton, *Phys. Rev. B* **1998**, *57*, 1505; b) Ü. Özgür, Y. I. Alivov, C. Liu, A. Teke, M. A. Reshchikov, S. Doğan, V. Avrutin, S.-J. Cho, H. Morkoç, *J. Appl. Phys.* **2005**, *98*, 041301.

[5] J. K. Nørskov, J. Rossmeisl, A. Logadottir, L. Lindqvist, J. R. Kitchin, T. Bligaard, H. Jonsson, *J. Phys. Chem. B* **2004**, *108*, 17886-17892.

[6] M. Li, L. Zhang, Q. Xu, J. Niu, Z. Xia, *J. Catal.* **2014**, *314*, 66-72.

[7] a) F. Calle-Vallejo, M. T. M. Koper, *Electrochim. Acta* **2012**, *84*, 3-11; b) H.-Y. Su, Y. Gorlin, I. C. Man, F. Calle-Vallejo, J. K. Nørskov, T. F. Jaramillo, J. Rossmeisl, *Phys. Chem. Chem. Phys.* **2012**, *14*, 14010-14022.

[8] X. Luo, G. Wang, Y. Huang, B. Wang, H. Yuan, H. Chen, *J. Phys. Chem. C* **2017**, *121*, 18534-18543.

[9] O. Piqué, F. Illas, F. Calle-Vallejo, *Phys. Chem. Chem. Phys.* **2020**, *22*, 6797-6803.